



Deposited via The University of Leeds.

White Rose Research Online URL for this paper:

<https://eprints.whiterose.ac.uk/id/eprint/122417/>

Version: Accepted Version

Proceedings Paper:

Van Alwon, J, Borman, D, Sleigh, A et al. (2017) Experimental and numerical modelling of aerated flows over stepped spillways. In: Proceedings of IAHR 2017. 37th IAHR World Congress, 13-18 Aug 2017, Kuala Lumpur, Malaysia. International Association for Hydro-Environment Engineering and Research (IAHR). ISSN: 2521-7119. EISSN: 2521-716X.

This conference paper is protected by copyright. This is an author produced version of a conference paper published in Proceedings of the 37th IAHR World Congress. Uploaded in accordance with the publisher's self-archiving policy.

Reuse

Items deposited in White Rose Research Online are protected by copyright, with all rights reserved unless indicated otherwise. They may be downloaded and/or printed for private study, or other acts as permitted by national copyright laws. The publisher or other rights holders may allow further reproduction and re-use of the full text version. This is indicated by the licence information on the White Rose Research Online record for the item.

Takedown

If you consider content in White Rose Research Online to be in breach of UK law, please notify us by emailing eprints@whiterose.ac.uk including the URL of the record and the reason for the withdrawal request.

EXPERIMENTAL AND NUMERICAL MODELLING OF AERATED FLOWS OVER STEPPED SPILLWAYS

JACOB VAN ALWON¹, DUNCAN BORMAN², ANDREW SLEIGH³ & NIK KAPUR⁴

¹ EPSRC Centre for Doctoral Training in Fluid Dynamics, University of Leeds, Leeds, UK
scjva@leeds.ac.uk

^(2,3) Institute for Public Health and Environmental Engineering (iPHEE), University of Leeds, Leeds, UK
d.j.borman@leeds.ac.uk; p.a.sleigh@leeds.ac.uk

⁴ Institute of Thermofluids, University of Leeds, Leeds, UK
n.kapur@leeds.ac.uk

ABSTRACT

Stepped spillways are a popular design choice for reservoir overflows due to the high rates of energy dissipation and air entrainment compared to smooth spillways. Air entrainment is important in spillway flows as it affects the pressures acting on the spillway surface, which in adverse conditions can damage the spillway. Air entrainment also causes flow bulking which increases the depth of flow. This study presents free surface and pressure data for aerated flows over an experimental stepped spillway, with pressures measured at different positions across the width of the channel. Within the step cavities recirculating vortices are observed in both the stream-wise and cross-stream directions, with the direction of circulation alternating at each subsequent step. These 3D effects cause the pressures acting on the step edges to vary across the width of the channel.

The Volume of Fluid (VOF) and Eulerian multiphase numerical models are used to predict flows over the spillway. The Eulerian multiphase model shows high levels of air entrainment and is able to predict the position of the free surface to reasonable accuracy. The VOF model, conversely, does not show any air entrainment and therefore under predicts the position of the free surface. The accuracy to which each numerical model predicts pressures on the step faces varies depending on the measurement location. Both of the numerical models accurately simulate the direction of circulation of the 3D vortices within the step cavities. Simulations with varying channel widths, conducted using the VOF model, show that the pattern of 3D vortices repeats as the channel width is increased.

Keywords: Stepped Spillway, Aeration, Multiphase Modelling.

1 INTRODUCTION

Stepped spillways dissipate significantly more energy than smooth spillways (Rice and Kadavy (1996), Christodoulou (1993) & Rajaratnam (1990)) and are therefore a popular design choice for reservoir overflows. The development of roller compacted concrete in the 1980s led to stepped spillways becoming an increasingly popular design choice for concrete spillways which increased research into the performance of such spillways. Masonry stepped spillway at embankment dams, however, have been common since the 18th century. The average age of dams in the UK is over 110 years (British Dam Society, 2006) so the inspection and maintenance of dams and spillways is of high importance.

Modelling has an important role to play in both design of new spillways and the inspection of existing infrastructure. Computational Fluid Dynamics (CFD) has the potential to provide an invaluable tool to model flows over stepped spillways. Current industry standard is to model spillways experimentally; however, CFD has certain advantages over physical modelling. For example, CFD allows the full scale spillway to be modelled so scale affects are not an issue. CFD models also allow any variable to be measured at any point in the domain so vulnerable areas or specific flow conditions can be identified. CFD models, however, are less well understood than physical models. Before CFD can be used in isolation to model high risk structures, such as reservoir spillways, they must be proven to accurately predict the important features of the flows being considered. Some important phenomena that need to be accounted for to varying extents are briefly discussed below.

Skimming Flow over Stepped Spillways: There are three flow regimes which occur over stepped spillways: nappe, transitional and skimming. For a given spillway geometry nappe flow occurs at low discharges, transitional flow occurs at moderate discharges and skimming flow occurs at high discharges (Chanson, 2002). This study focusses solely on the skimming flow regime. The characteristics of skimming flow has been described by many authors, including Chamani and Rajaratnam (1999), Chanson (1994) Rajaratnam (1990) and Sorensen (1985). During skimming flow the bulk of the flow “skims” over the steps and recirculating vortices are formed in the step cavities (figure 1). The step edges form a pseudo-bottom which

separates the recirculating vortices and the bulk of the flow. The interaction between the spillways surface and the flow creates turbulence and a boundary layer forms. Moving downstream the boundary layer increases in depth until it meets the free surface at which point free surface aeration begins. This is known as the point of inception. Downstream of the inception point is a region of gradually varied flow. Air bubbles are transported to the pseudo-bottom and into the step cavities. The entrained air causes flow bulking, increasing the depth of flow. This is an important factor in the design of the spillway sidewalls as overtopping must be prevented. Further downstream a uniform flow region is formed where the depth of flow, velocity profiles and air concentration remain relatively constant. Skimming flow is an efficient means of energy dissipation, with the primary dissipation mechanism being the transfer of shear stress from the bulk flow to maintain the recirculating vortices. Some energy is also dissipated through turbulence in the aerated region.

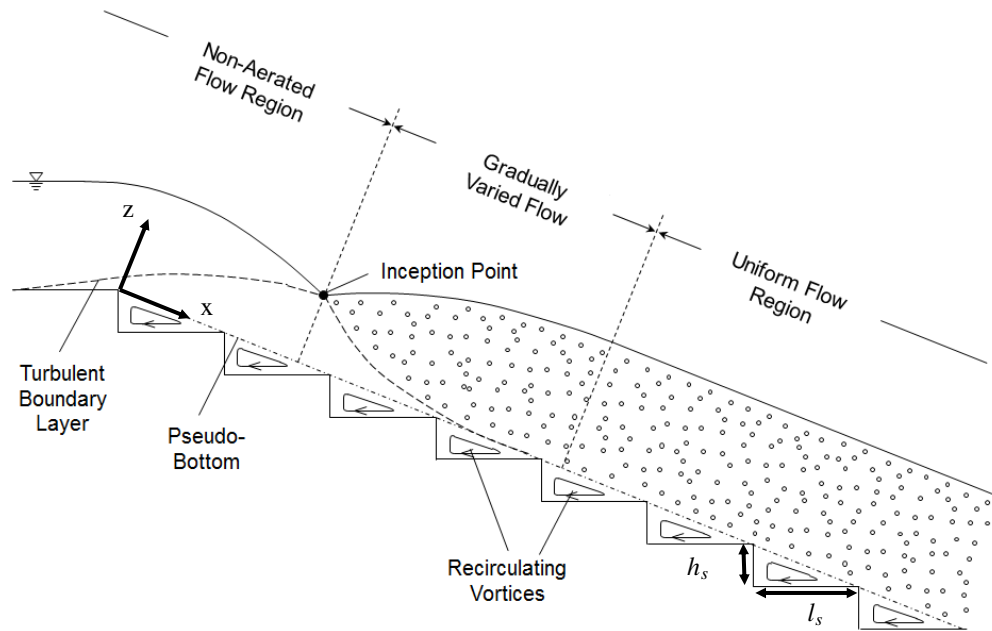


Figure 1. Skimming flow over a stepped spillway identifying key flow features such as the inception point, recirculating vortices and air entrainment.

Pressure effects: Under skimming flow conditions stepped spillways are subjected to large variations in pressure. Zhang et al. (2012), Sánchez-Juny et al. (2007) & Sánchez-Juny et al. (2000) show that high pressures occur at the downstream end of the horizontal step edge and the bottom of the vertical step edge, where the recirculating vortex impinges on the step. The upstream end of the horizontal step edge and the top of the vertical step edge are subject to lower pressures where flow separation occurs. These studies, and others, including Zhang and Chanson (2016), Xu (2015) and Matos et al. (1999), have all taken pressure measurements at the centreline of the spillway. This study investigates the variation in pressure across the width of the spillway channel.

Plucking: In masonry spillways large pressure gradients can develop between the front of blocks, where flows cause low pressures, and the back of blocks, where backing material exerts a lateral earth pressure. This pressure gradient can cause blocks to be plucked from the spillway into the flow, leaving a gap in the spillway surface or sidewall. This gap allows water to ingress behind the spillway, causing erosion of backing material which can lead to failure of the spillway. This is particularly hazardous at earthen fill dams as the spillway often runs down the mitre of the dam so ingress of water could cause erosion of the dam itself. Two high profile spillway failures in the UK occurred at the Boltby reservoir in 2005 and the Ulley reservoir in 2007 due to failure of the spillway sidewalls. It is thought that one of the failure mechanisms of the Ulley spillway was due to plucking of masonry blocks from the sidewall (Hinks et al, 2008) Missing blocks were also observed in the sidewall of the Boltby spillway (Mason and Hinks, 2008). Following these failures the UK Environment Agency commissioned a detailed study into the safety of masonry stepped spillways which is described by Winter et al. (2010). Some key findings of the study are that small areas of damage to the spillway can further increase the risk of plucking and that localised variations in pressure are an important factor in the removal of masonry blocks.

Cavitation: Plucking does not occur on concrete spillways however consideration must be given to cavitation damage. Cavitation is the process by which the local pressure falls below the vapour pressure of the liquid causing the liquid to vaporise and form bubbles. When these bubbles are transported to an area of

higher pressure they collapse and produce extremely high localised pressures which can damage solid boundaries. There are no recorded cases of cavitation damage being observed on stepped spillways. Frizell et al (2012) claim that this is due to conservative designs preventing the conditions which could produce cavitation from occurring. Chanson (2002) claims, however, that there is no risk of cavitation damage to stepped spillways due to slower flow velocities and greater water depths producing a cavitation index 10 to 100 greater than on smooth spillways with identical discharges.

Air Entrainment: Air entrainment is known to significantly reduce the risk of cavitation damage. Experiments conducted by Dong et al (2010) and McGee (1988) show that air entrainment prevents the low pressures which cause cavitation from occurring. As both cavitation and plucking occur in low pressures regions, it follows that air entrainment would also reduce the risk of plucking in masonry spillways. This, however, leaves the non-aerated flow region at risk to plucking and possibly cavitation damage. One of the most challenging areas to model numerically is the air entrainment, and the resulting flow behaviour.

2 EXPERIMENTAL SETUP

Experiments are conducted in the spillway shown in figure 2 (a). The spillway channel is 150 mm wide and consists of 15 steps with $h_s = 80$ mm and $l_s = 80$ mm. The spillway crest is curved to prevent the flow from jetting over the steps. Pressures are recorded at steps 2, 5 and 12 using an Omega PX409 pressure transducer with a measurement range of atmospheric pressure ± 6894.8 Pa. At each step pressures are measured at four points on the horizontal step face and four points on the vertical step face. In each case there are two measurement points along the centreline of the spillway and two points 20 mm from the wall of the spillway. This will allow any variation in pressure across the channel width to be identified.

To measure the position of the free surface the side elevation of the spillway was digitally photographed using a 13 – megapixel digital camera. The position of the free surface is then automatically calculated using image processing analysis of the images using the computation and visualization software MATLAB.

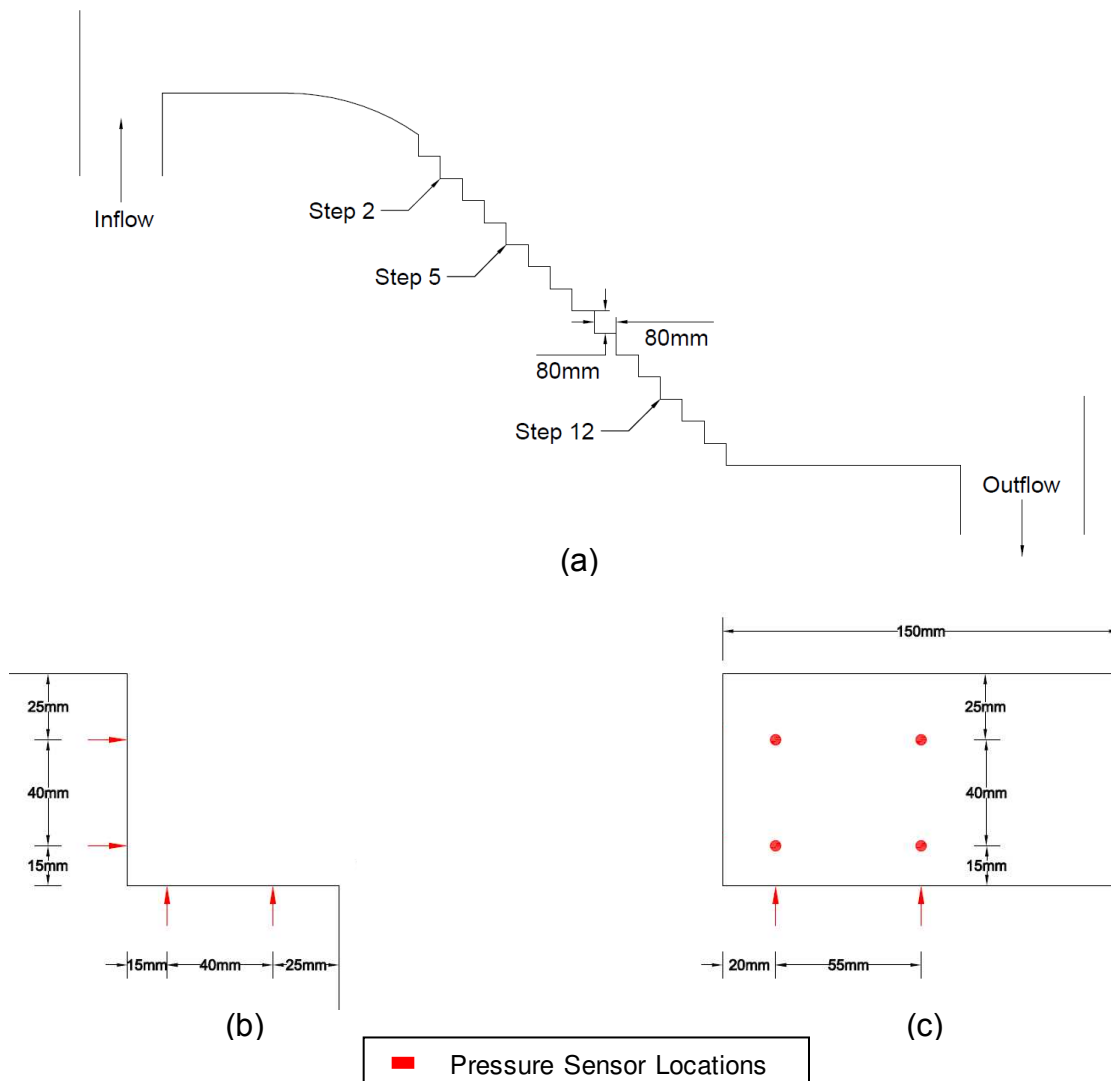


Figure 2. (a) Experimental spillway (b) Step profile (c) Vertical step face.

3 NUMERICAL MODELLING

3.1 Numerical Models

Volume of Fluid (VOF) Model: The VOF model is a multiphase model first proposed by Hirt and Nichols (1981). The model assumes that all fluids are immiscible and is generally used where the interface between fluids is important. A single set of momentum equations are solved for all phases and the volume fraction of each fluid in a cell is tracked. The volume fraction of each secondary phase is calculated using a volume fraction equation based on the continuity equation

$$\frac{\partial}{\partial t} (\alpha_k) + \nabla \cdot (\alpha_k \mathbf{u}_k) = \Gamma_k \quad [1]$$

where the subscript k denotes phase k , α is the volume fraction, \mathbf{u} is the velocity and Γ is the mass generation. The volume fraction of the primary phase is calculated based on

$$\sum_{k=1}^n \alpha_k = 1 \quad [2]$$

The following single momentum equation is then solved for all phases

$$\rho \frac{D\mathbf{u}}{Dt} = -\nabla p + \nabla \cdot (\boldsymbol{\tau} + \boldsymbol{\tau}^T) + \rho \mathbf{g} + \mathbf{F}_s \quad [3]$$

where ρ is the average density of all phases, p is the pressure, $\boldsymbol{\tau}$ is the viscous stress tensor, $\boldsymbol{\tau}^T$ is the turbulent stress tensor and \mathbf{F}_s is the surface tension. The average density is calculated by

$$\rho = \sum_{k=1}^n (\alpha_k \rho_k) \quad [4]$$

The average viscosity is calculated in the same manner.

The VOF model does not allow phases to interpenetrate so therefore is limited to the extents that it can predict air entrainment. Despite this, several studies have been shown to be able to accurately predict certain characteristics of skimming flow over stepped spillways. Chen et al (2002) used the VOF model to simulating skimming flow over a spillway with $h_s = 60$ mm and $l_s = 45$ mm. Reasonable predictions of velocity profiles and pressures acting on the step edges are made. Chakib (2013) used the VOF model to accurately predict velocity profiles at several locations. The numerical results show air entrainment along the chute. As the VOF model does not allow phases to interpenetrate, it is unclear how this result is achieved. Kositgittiwong et al. (2013) modelled a large scale experimental spillway with 25 steps of 1220 mm length and 610 mm height. Velocity profiles are accurately predicted in both the aerated and non-aerated regions. Bombardelli et al (2011) used the TruVOF method, which is part of the commercial CFD package Flow-3D, to investigate the non-aerated region. In the TruVOF method only the liquid phase is modelled. Good predictions of the velocity profiles, water depth and the depth of the turbulent boundary layer were made. Valero and Bung (2015) also used the one fluid approach in Flow-3D, this time with an air entrainment model included. Air entrainment and flow bulking were observed; however, the air entrainment, and therefore flow depth in the aerated region, was overestimated. This was attributed to calibration parameters used for smooth spillways not producing accurate results for stepped spillways. Borman et al. (2015) used the VOF model to accurately predict the location of the free surface of waves and hydraulic jumps in a full scale recreational white water course. In the study the physical free surface was measured using laser scanning of white water, which is associated with air entrainment.

Eulerian Multiphase Model: The Eulerian multiphase model is described by Ishii and Hibiki (2010). In the model phases interact with one another and one phase may become dispersed in another. Each phase is considered separately and therefore a set of conservation equations must be solved for each phase. For phase k the continuity equation is

$$\frac{\partial}{\partial t} (\alpha_k \rho_k) + \nabla \cdot (\alpha_k \rho_k \mathbf{u}_k) = \Gamma_k \quad [5]$$

and the momentum equation is

$$\alpha_k \rho_k \frac{D_k \mathbf{u}_k}{Dt} = -\alpha_k \nabla p + \nabla \cdot [\alpha_k (\boldsymbol{\tau}_k + \boldsymbol{\tau}_k^T)] + \alpha_k \rho_k \mathbf{g} + M_k \quad [6]$$

where M is the momentum transfer from the phase interface. The interaction between phases is controlled by the terms Γ and M and depends on the density of the dispersed phase, the diameter of the dispersed droplets or bubbles, the viscosity of the continuous phase, the interfacial area and the drag function.

Studies into free surface aeration modelling using the Eulerian multiphase model are relatively scarce. Cheng and Chen (2011) modelled a hydraulic jump using the Eulerian multiphase method. The air volume fraction, free surface position and velocity profiles were all accurately predicted. The use of the VOF model to model skimming flow over stepped spillways has been relatively well studied, however the model has limitations as it is unable to simulate air entrainment. The Eulerian multiphase model has the potential to predict free surface aeration over stepped spillways, however the model's accuracy and reliability is not proven. This study investigates the Eulerian multiphase model's ability to predict air entrainment, and pressure profiles in skimming flow over stepped spillways and uses the VOF model as a benchmark for comparison.

3.2 Numerical Modelling Procedure

Numerical modelling was conducted using the CFD package ANSYS Fluent v16.2. All simulations were conducted in 3D using the Realizable $k-\epsilon$ turbulence model and run transiently until a steady state solution was achieved. A symmetry boundary condition was used at the centreline of the spillway to reduce the size of the computational domain and still simulate the entire spillway. A structured quadrilateral mesh was used with each step containing 40 by 40 by 40 cells. Presented CFD results have been verified to be independent of the grid resolution.

4 RESULTS AND DISCUSSION

4.1 Flow Characteristics

Experimental Model Results: The spillway was tested under a flow rate of 15 l/s. Figure 3 (a) clearly shows the non-aerated region, inception point, gradually varied flow region and uniform flow region. Upstream of the uniform region the flow is unsteady. The location of the point of inception is not static in location over time, but fluctuates around a mean position by up to two steps in either direction. Figure 3 (a) shows the inception point at approximately its average position. Strong free surface aeration is observed downstream of the inception point which increases the flow depth due to flow bulking. In the gradually varied flow region there is intense splashing and the free surface position fluctuates almost constantly. The depth of flow perpendicular to the pseudo bottom is highest in the gradually varied flow region and settles to a slightly lower level in the uniform flow region.

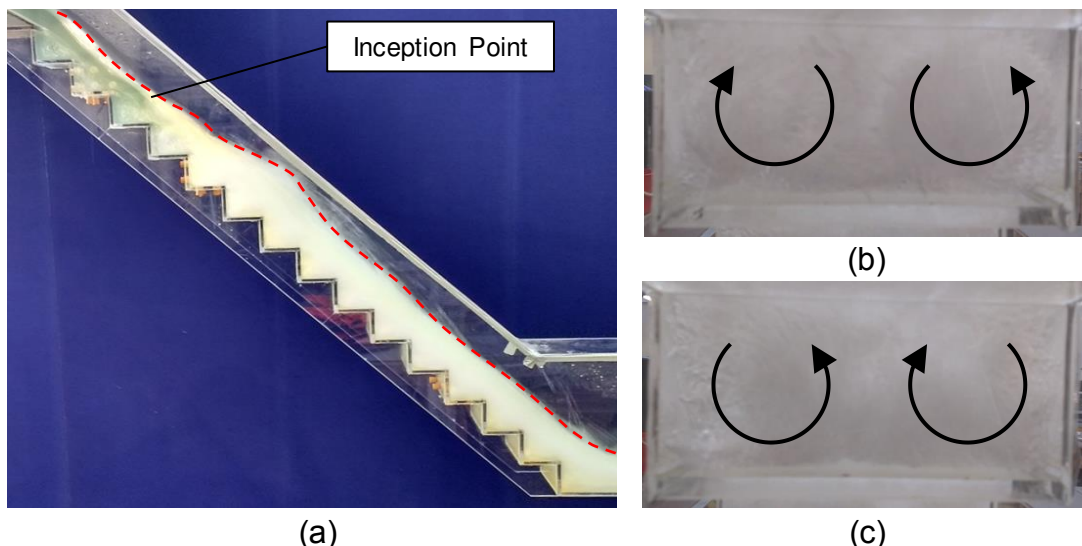


Figure 3. (a) Experimental Spillway (b) & (c) Cross-stream Vortices

As well as the stream-wise recirculating vortices shown in figure 1, further cross-stream vortices can be observed in the step cavities, recirculating perpendicular to the main flow direction. In each step there are two vortices, circulating in opposite directions and interacting at the centreline of the spillway. The vortices circulate in one of two directions. Either the vortices flow upwards at the wall and impinge on the horizontal step face at the centre (figure 3 (b)), or the vortices impinge at the wall and flow upwards at the centreline (figure 3 (c)). The direction of circulation changes at each step, with the odd numbered steps resembling figure 3 (b) and the even numbered steps resembling figure 3 (c). Matos et al. (1999) reports that the recirculating vortices in the step cavities exhibit 3D behaviour, however the detailed structure of the vortices is not described.

Numerical Model Results: Figure 4 shows contours of air volume fraction predicted at the centre plane of the spillway for the Eulerian and VOF models. It can be seen that the VOF model shows no air entrainment or inception point. The Eulerian model shows high levels of free surface aeration and resembles the experiments more closely. Defining the inception point as the location where air begins to be entrained into the flow, the Eulerian model shows the inception point at approximately the crest of the spillway. It can be seen from figure 3 (a) that this is not the case and the average position of the inception point is around step four. Air appears to be transported into the step cavities slightly further upstream than in the Eulerian model. However, to accurately validate the volume of air entrained in the Eulerian model, measurements of air concentrations in the physical model are required.

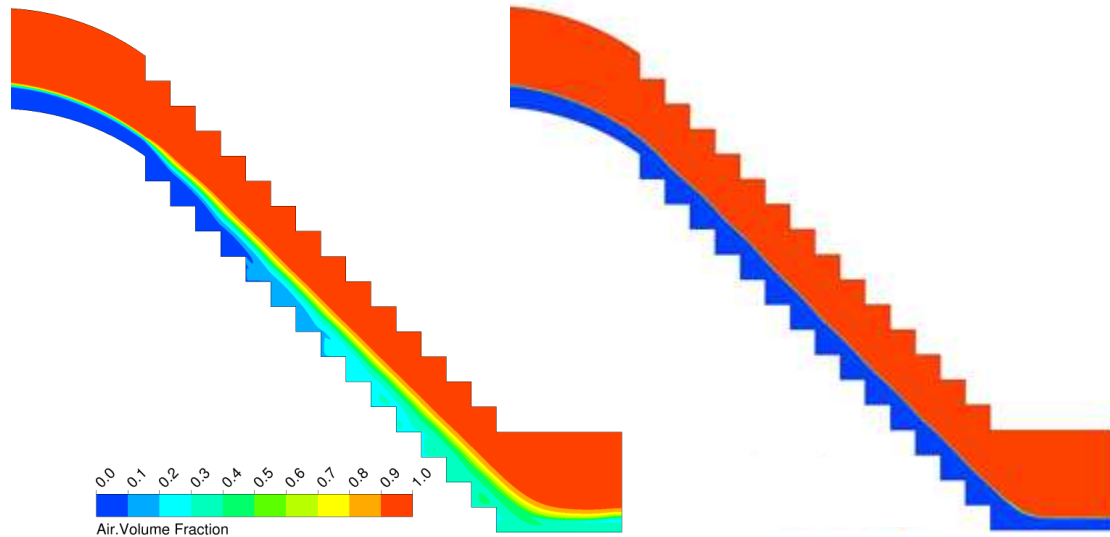


Figure 4. Air volume fraction for (a) Eulerian model (b) VOF model.

4.2 Free Surface Location

The red dashed lines in figure 3 (a) shows the position of the free surface. This is calculated using image processing routines in MATLAB (based on the boundary between the darker coloured background and the lighter coloured water). In the numerical models the free surface has been defined as the depth at which the air concentration = 90%.

Figure 5 shows the experimental and numerical free surface levels perpendicular to the pseudo-bottom, where x is the distance along the pseudo-bottom from the spillway crest and z is the perpendicular distance from the pseudo-bottom. The inception point and subsequent increase in depth can be seen followed by the slight decrease in depth at the uniform flow region. The Eulerian model shows generally good agreement, with the free surface elevation being under predicted in the unsteady flow region and slightly over predicted in the uniform flow region. The Eulerian model shows a smooth free surface whereas the experimental data shows that free surface is uneven. The VOF model under predicts the free surface at all locations. This is due to the fact that in the VOF model no air is entrained into the flow so flow bulking is not predicted.

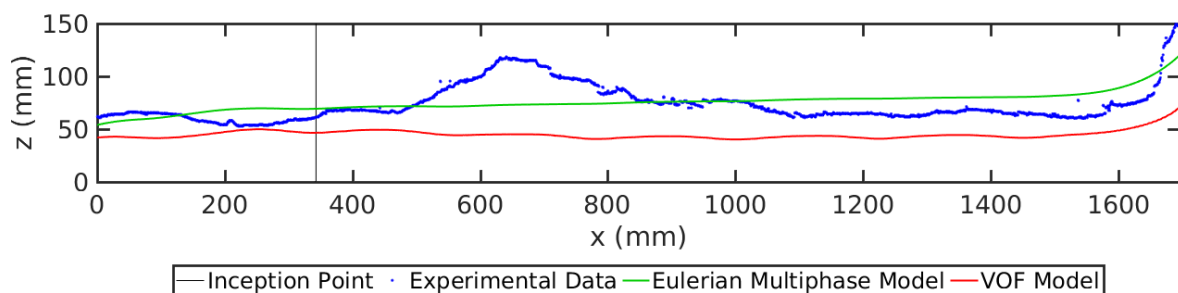


Figure 5. Experimental and numerical free surface depths perpendicular to the pseudo-bottom.

4.3 Pressure Measurements

Pressures were measured in the experimental spillway at a sampling rate of 1 kHz for 30 seconds. All pressure data presented represents the mean pressure relative to atmospheric pressure. The locations of the pressure data presented are detailed in figures 2 (b) & (c). Figures 6 and 7 show the experimental and numerical pressures on the horizontal and vertical step faces respectively. The left hand plots show the pressures at the centreline of the spillway and the right hand plots show the pressures 20 mm from the spillway wall. Figure 8 shows the contours of pressure on the horizontal and vertical step faces for both models. The experimental mean pressures are superimposed onto the contours in the corresponding locations.

On the horizontal step faces, the experimental data shows that the expected pressure profile, with the highest pressure at the downstream end of the step, can be seen close to the wall at steps two and twelve. At the centreline of these steps, however, the expected pressure profile is not seen and there is little variation in pressure between the upstream and downstream ends of the step face. This pressure pattern corresponds to the direction of circulation of the cross stream vortices. At steps two and twelve, the cross-stream vortices impinge on the step face close to the wall of the spillway, where the expected pressure profile occurs. At the centreline of these steps the cross stream vortices flow away from the horizontal step face and the expected pressure profile does not occur. At step five the cross stream vortices circulate in the opposite direction and the opposite pattern of pressure can be seen.

At the vertical step faces there is much less variation in the pressure profiles across the width of the channel, and in all cases the expected pressure profile is observed, with the lowest pressures occurring at the top of the step. There is still, however, some variation in the pressures across the width of the channel which correspond to the direction of circulation of the cross-stream vortices. At steps two and twelve the pressures are slightly lower close to the wall and at step five the pressures are slightly lower at the centreline.

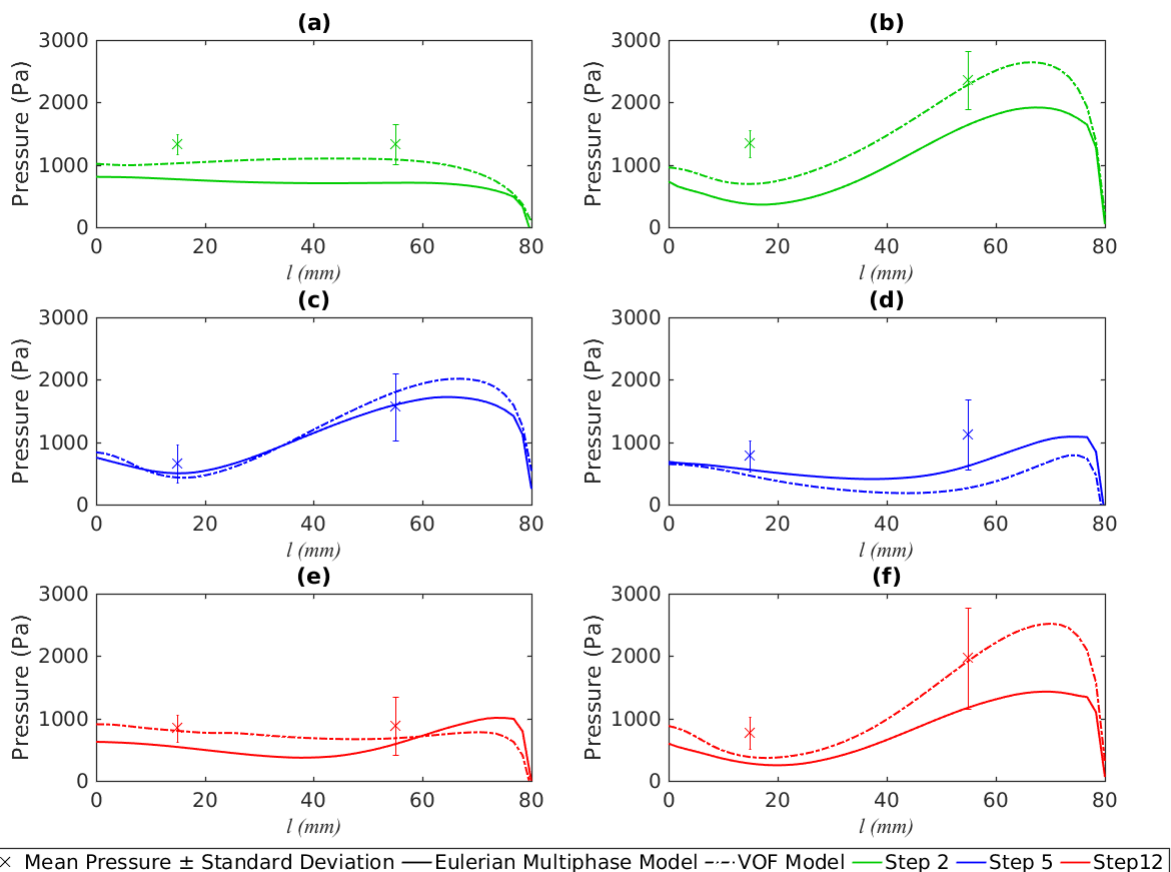


Figure 6. Experimental and numerical pressures acting on the horizontal step faces (a), (c) & (d) at the centreline of the spillway (b), (d) & (f) 20 mm from the spillway wall.

At the horizontal step faces both the Eulerian and VOF models show the same general profile as the experimental data, with the variations in pressure across the width of the channel corresponding to the direction of circulation of the cross stream vortices. At step two the VOF model performs better than the Eulerian model, with the Eulerian model underestimating the pressure at all positions. This is not surprising as step two lies within the unaerated region. The VOF model does not predict aeration; however, as can be seen in figure 4, some air entrainment occurs above step two in the Eulerian model. The VOF model is accurate at

the downstream end of the step, however also underestimates the pressure at the upstream end of the step. At step five both models perform well at the centreline of spillway; however the Eulerian model predicts the pressures more accurately close to the wall. At step twelve the Eulerian model predicts the pressures reasonably well at the downstream end of the step, however underestimates the pressures at the upstream end of the step. The VOF model performs more accurately than the Eulerian model however underestimates the pressure at the upstream end of the step close to the wall.

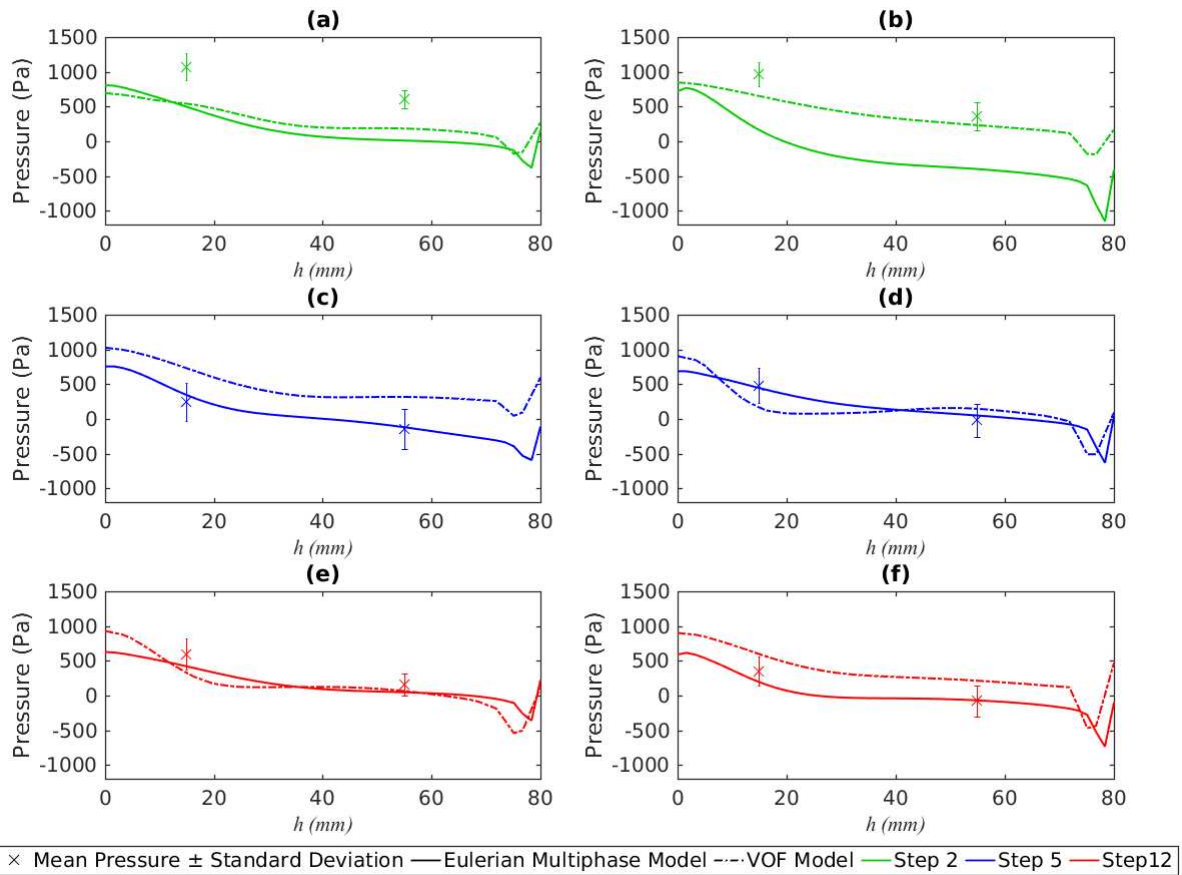


Figure 7. Experimental and numerical pressures acting on the vertical step faces (a), (c) & (d) at the centreline of the spillway (b), (d) & (f) 20 mm from the spillway wall.

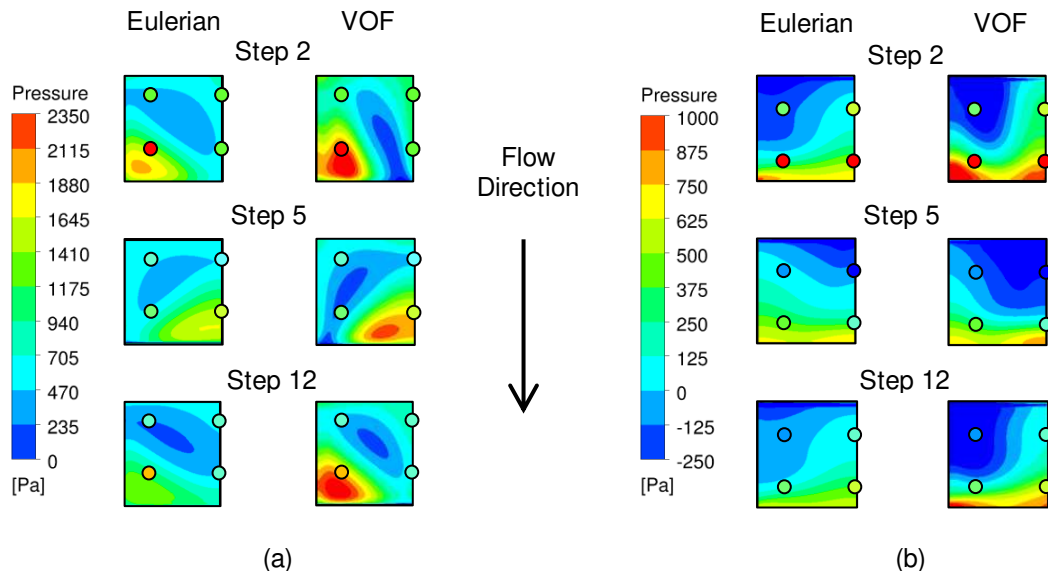


Figure 8. Numerical contours of pressure with experimental mean pressures superimposed in the corresponding locations. (a) Horizontal step faces. (b) Vertical step faces.

At the vertical step faces the two numerical models also show the same general pressure profiles as the experimental data. At step two the Eulerian model underestimates the pressure at all positions. The VOF model performs slightly better than the Eulerian model, however, still underestimates the pressure at the centreline and at the bottom of the step face close to the wall. At steps five and twelve the Eulerian model accurately predicts the pressure in all locations. The VOF model performs well at step five close to the wall and step twelve at the centreline. It can be seen that the largest variation between the Eulerian and VOF pressure profiles are at the centreline of step five and close to the walls of steps two and twelve. It is at these locations across the channel width, where the cross stream vortices impinge on the horizontal step face. Increased turbulence in these regions may be the reason for the variation between the two numerical models.

4.4 3D Vortex Structures

Figure 9 shows the stream-lines over steps three and four and the pressure contours on the step faces for the Eulerian and VOF models. The streamlines have been seeded close to the step corner in each step cavity. In both the Eulerian and VOF models two separate vortices which meet at the centre of the channel can be seen. The direction of circulation of these vortices changes at each subsequent step so that they impinge on the horizontal step face either at the centre of the spillway or close to the walls, matching the directions that are observed in the physical model.

It can be seen from figure 9 that there is no distinction between a cross-stream vortex and a stream-wise vortex and in fact there is only one three-dimensional vortex in each half of a step cavity. The axis of this vortex runs diagonally downstream from either the centre of the spillway to the wall, or the wall to the centre, depending on which step is being considered. The variations in pressure across the width of the horizontal step faces match the direction of these vortices closely, with the highest pressures occurring where the vortices impinge on the step face. On the vertical step faces, the lower pressure regions correspond to the position where the axes of the vortices meet the step face.

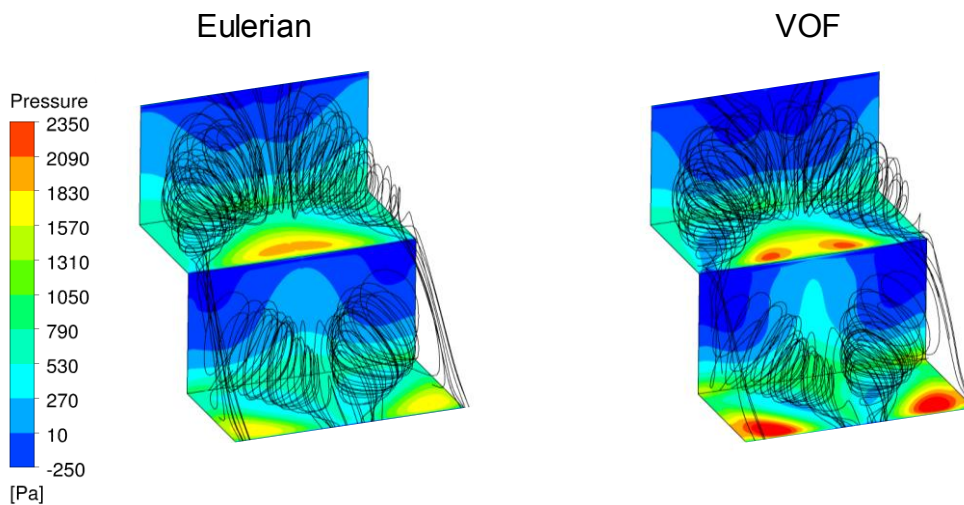


Figure 9. Pressure contours and streamlines at steps three and four.

The width of the experimental spillway is relatively narrow compared to prototype spillways and also provides a ratio of channel width to step height (or length) of 1.875:1. As this is almost 2:1 and two vortices occur across the step width, it was considered that the aspect ratio of channel width to step height or length may be the cause of the observed vortices. In an attempt to determine whether the vortices occurred due to the narrow channel width, or the ratio of width to step height, simulations were conducted of spillways with varying channel widths. The simulations were conducted using the VOF model as the computational cost is significantly less than the Eulerian model, due to only a single momentum equation being solved. The VOF model has been shown to produce the same flow and pressure patterns that are observed in the experimental spillway so can be used to simulate channels of varying width with reasonable confidence.

Figure 10 (a) shows the stream-lines and pressure profiles at steps three and four of a channel of 300 mm width, double that of the experimental spillway. As with the previous cases, the simulation was conducted with a symmetry boundary condition at the centre of the spillway. It can be seen that the vortex structure observed in the simulations of the 150 mm wide spillway is repeated, so that there are 4 vortices rather than two. Again the direction of the vortices changes at each subsequent step and the pressure profiles correspond to the direction of circulation of the vortices. This pattern can also be seen for channel widths of 450 mm, producing six vortices, and 600 mm, producing eight vortices.

In figure 10 (b) a symmetry boundary condition has been used at both of the walls of the spillway, essentially giving the spillway an infinite width. Again the repeating pattern of vortices and the corresponding

pressure profiles can be seen. This shows that the vortex structures which are observed are not caused by the interaction between the fluid and the walls.

This pattern of repeating vortices, which change direction at each subsequent step, shows some resemblance to those described by Lopes et al. (2017). In this study, however, the repeating vortex structure only occurred with a channel width of 500 mm. With a channel width of 300 mm the flow appeared to be relatively uniform across the width of the channel and at each subsequent step. The numerical data presented in this study shows that the occurrence of these vortices does not depend on the width of the channel. The work by Lopes et al. (2017) is conducted on a spillway with a ratio of l to h of 2:1 rather than 1:1 in this study. This difference may account for why different behaviours are observed for varying channel widths.

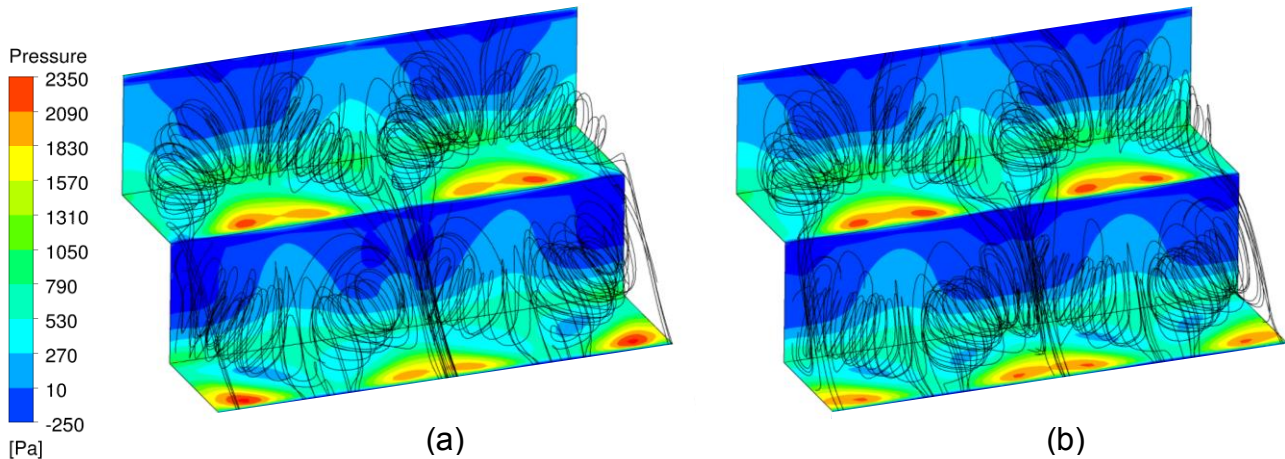


Figure 10. Pressure contours and streamlines at steps three and four for (a) a channel width of 300 mm (b) and infinite channel width.

5 CONCLUSIONS

This study presents free surface and pressure data for an experimental stepped spillway and the corresponding numerical data for two multiphase models. As well as the stream-wise recirculating vortices described by many authors, cross-stream vortices are also observed in the step cavities. The direction of circulation of these vortices changes at each step. These 3D flow patterns cause the pressures acting on the step faces to vary along the width of the chute.

The Eulerian multiphase model is able to reasonably predict the position of the free surface over the steps and shows aeration of the flow. The VOF model, however, does not show any air entrainment and therefore the free surface depth is under predicted. Both of the numerical models predict the correct general pattern of pressure as it varies across the channel width. The performance of each model varies depending on the measurement location. The Eulerian model generally predicts pressures accurately in the aerated region but underestimates the pressures in the non-aerated region, where the VOF model is more accurate. The VOF model predicts the pressures in the aerated region well in some locations, but less well in others.

Both of the numerical models accurately simulate the pattern of two 3D vortices in each step cavity, which change direction at each step. The VOF model was used to simulate spillways of increasing channel width, and this vortex pattern was found to repeat as the channel width increases. The vortex pattern was also found for a channel with symmetry boundary conditions at the two walls. This shows that the vortices are not caused by the interaction of the fluid and the walls.

ACKNOWLEDGEMENTS

This work was funded by EPSRC [grant number EP/L01615X/1]. The authors would also like to thank Hydrotec Consultants Ltd for constructing the spillway in which experiments were conducted.

REFERENCES

- Amador A., Sánchez-Juny, M & Dolz J. (2009) Developing flow region and pressure fluctuations on steeply sloping stepped spillways. *Journal of Hydraulic Engineering*, 135(12):1092–1100.
- Bombardelli, F.A., Meireles, I., & Matos, J. (2011). Laboratory measurements and multi-block numerical simulations of the mean flow and turbulence in the non-aerated skimming flow region of steep stepped spillways. *Environmental Fluid Mechanics*, 11(3), 263-288.
- Borman, D., Sleigh, P.A., & Coughtrie, A. (2015). Three dimensional free-surface modelling with a novel validation approach. *E-proceedings of the 36th IAHR World Congress*. Leeds.
- British Dam Society (2006). Improvements in Reservoir Construction, Operation and Maintenance. *Proceedings of the 14th Conference of the British Dam Society*, Thomas Telford.
- Chakib, B. (2013). Numerical computation of inception point location for flat-sloped stepped spillway. *International Journal of Hydraulic Engineering*, 2(3), 47-52.
- Chamani, M.R., & Rajaratnam, N. (1999). Characteristics of skimming flow over stepped spillways. *Journal of Hydraulic Engineering*, 125(4), 361-368.
- Chanson, H. (1994). Hydraulics of skimming flows over stepped channels and spillways. *Journal of Hydraulic Research*, 32(3), 445-460.
- Chanson, H. (2002). *Hydraulics of stepped chutes and spillways*. CRC Press.
- Chen, Q., Dai, G., & Liu, H. (2002). Volume of fluid model for turbulence numerical simulation of stepped spillway overflow. *Journal of Hydraulic Engineering*, 128(7), 683-688.
- Cheng, X.J., & Chen, X.W. (2011). Applying Improved Eulerian Model for Simulation of Air-Water Flow in a Hydraulic Jump. *World Environmental and Water Resources Congress 2011: Bearing Knowledge for Sustainability* (pp. 3882-3896).
- Christodoulou, G. C. (1993). Energy dissipation on stepped spillways. *Journal of Hydraulic Engineering*, 119(5), 644-650.
- Dong, Z., Wu, Y., & Zhang, D. (2010). Cavitation characteristics of offset-into-flow and effect of aeration. *Journal of hydraulic research*, 48(1), 74-80.
- Frizell, K.W., Renna, F.M., & Matos, J. (2012). Cavitation potential of flow on stepped spillways. *Journal of Hydraulic Engineering*, 139(6), 630-636.
- Hinks, J.L., Mason, P.J., & Claydon, J.R. (2008). Ulley Reservoir and high velocity spillway flows. *Ensuring reservoir safety into the future: Proceedings of the 15th Conference of the British Dam Society* (pp. 227-237). Thomas Telford Publishing.
- Hirt, C.W., & Nichols, B.D. (1981). Volume of fluid (VOF) method for the dynamics of free boundaries. *Journal of computational physics*, 39(1), 201-225.
- Ishii, M., & Hibiki, T. (2010). *Thermo-fluid dynamics of two-phase flow*. Springer Science & Business Media.
- Kositgittiwong, D., Chinnarasri, C., & Julien, P.Y. (2013). Numerical simulation of flow velocity profiles along a stepped spillway. *Proceedings of the Institution of Mechanical Engineers, Part E: Journal of Process Mechanical Engineering*, 227(4), 327-335.
- Lopes, P., Leandro, J., Carvalho, R.F., & Bung, D.B. (2017). Alternating skimming flow over a stepped spillway. *Environmental Fluid Mechanics*, 1-20.
- Mason, P.J., & Hinks, J.L. (2008). Security of stepped masonry spillways: lessons from Ulley dam. *Dams and Reservoirs*, 18(1), 5-8.
- Matos, J., Sánchez, M., Quintela, A., & Dolz, J. (1999). Characteristic depth and pressure profiles in skimming flow over stepped spillways. *Congress IAHR*, (Vol. 28).

- McGee, R.G. (1988). Prototype evaluation of Libby dam sluiceway aeration system. *Model-Prototype Correlation of Hydraulic Structures*, 138–147. ASCE.
- Rajaratnam, N. (1990). Skimming flow in stepped spillways. *Journal of Hydraulic Engineering*, 116(4), 587-591.
- Rice, C.E., & Kadavy, K.C. (1996). Model study of a roller compacted concrete stepped spillway. *Journal of Hydraulic Engineering*, 122(6), 292-297.
- Sánchez-Juny, M., Bladé, E., & Dolz, J. (2007). Pressures on a stepped spillway. *Journal of Hydraulic Research*, 45(4), 505-511.
- Sánchez-Juny, M. S., Pomares, J., & Dolz, J. (2000, March). Pressure field in skimming flow over a stepped spillway. *Proceedings of the International Workshop on Hydraulics of Stepped Spillways, Zurich. Edited by HE Minor and WH Hager*. AA Balkema, Rotterdam (pp. 137-146).
- Sorensen, R.M. (1985). Stepped spillway hydraulic model investigation. *Journal of Hydraulic Engineering*, 111(12), 1461-1472.
- Valero, D., & Bung, D. B. (2015, June). Hybrid investigations of air transport processes in moderately sloped stepped spillway flows. *E-Proceedings of the 36th IAHR World Congress (Vol. 28)*.
- Winter, C., Mason, P., Baker, R., & Ferguson, A. (2010). Guidance for the Design and Maintenance of Stepped Masonry Spillways. *Environment Agency, London, Report SC080015*.
- Xu, W., Luo, S., Zheng, Q., & Luo, J. (2015). Experimental study on pressure and aeration characteristics in stepped chute flows. *Science China Technological Sciences*, 58(4), 720-726.
- Zhang, G., & Chanson, H. (2016). Hydraulics of the developing flow region of stepped spillways. II: Pressure and velocity fields. *Journal of Hydraulic Engineering*, 142(7), 04016016.
- Zhang, J., Chen, J., & Wang, Y. (2012). Experimental study on time-averaged pressures in stepped spillway. *Journal of Hydraulic Research*, 50(2), 236-240.